Chemical Engineering Science 122 (2015) 360–372

Contents lists available at ScienceDirect

Chemical Engineering Science

journal homepage: www.elsevier.com/locate/ces

Modelling and optimisation of the one-pot, multi-enzymatic synthesis of chiral amino-alcohols based on microscale kinetic parameter determination ☆

L. Rios-Solis [a], P. Morris [a], C. Grant [a], A.O.O. Odeleye [a], H.C. Hailes [b], J.M. Ward [a], P.A. Dalby [a], F. Baganz [a], G.J. Lye [a,*]

[a] The Advanced Centre for Biochemical Engineering, Department of Biochemical Engineering, University College London, Torrington Place, London, WC1E 7JE, UK
[b] Department of Chemistry, University College London, 20 Gordon Street, London,WC1H 0AJ, UK

HIGHLIGHTS

- Integration of numerical methods and microscale tools for kinetic characterisation.
- Synthetic biology principles for 'mix and match' expression of pairs of enzymes.
- Model predictions for the multi-enzymatic syntheses were verified experimentally.
- Reaction simulations were used to identify key process bottlenecks.
- Optimum conditions for fed-batch bioreactor operation were identified.

ARTICLE INFO

Article history:
Received 21 June 2014
Received in revised form
4 September 2014
Accepted 25 September 2014
Available online 5 October 2014

Keywords:
Transketolase
Transaminase
One-pot synthesis
Synthetic biology
Chiral amino-alcohols
Scale-up
Kinetic modelling

ABSTRACT

Advances in synthetic biology are facilitating the *de novo* design of complex, multi-step enzymatic conversions for industrial organic synthesis. This work describes the integration of multi-step enzymatic pathway construction with enzyme kinetics and bioreactor modelling, in order to optimise the synthesis of chiral amino-alcohols using engineered *Escherichia coli* transketolases (TK) and the *Chromobacterium violaceum* transaminase (TAm). The specific target products were (2*S*,3*S*)-2-aminopentane-1,3-diol (APD) and (2*S*,3*R*)-2-amino-1,3,4-butanetriol (ABT). Kinetic models and parameters for each of the enzymatic steps were first obtained using automated microwell experiments. These identified the TK-catalysed conversions as being up to 25 times faster than the subsequent TAm conversions and inhibition of TAm by the amino-donor used, (*S*)-(−)-α-methylbenzylamine (MBA), as limiting the overall conversion yields. In order to better 'match' the relative rates of the two enzymes an *E. coli* expression system, based on two compatible plasmids, was constructed to produce both enzymes in a single host. By control of induction time and temperature it was possible to produce six times more recombinant TAm than TK to help balance the reaction rates. To overcome MBA inhibition and an unfavourable reaction equilibrium, fed-batch addition of the amino-donor was introduced as well as the use of isopropylamine as an alternate amino-donor. Adopting these strategies, and using the kinetic models to optimise feeding strategies, the one pot syntheses of APD and ABT were successfully scaled-up to preparative scales. Excellent agreement was found between the kinetic profiles and yields predicted and those achieved experimentally at the larger scale. In this case the integration of these multi-disciplinary approaches enabled us to achieve up to a 6 fold greater yield using concentrations an order of magnitude higher than in previous preparative scale batch bioconversions carried out sequentially.

1. Introduction

With the recent advances in synthetic biology (McArthur and Fong, 2010), there is increasing interest in the design of multi-step enzymatic conversions for the synthesis of speciality chemicals and pharmaceutical intermediates. Irrespective of whether such *de*

☆Manuscript prepared for Chemical Engineering Science (June 2014).

* Corresponding author.
E-mail address: g.lye@ucl.ac.uk (G.J. Lye).

http://dx.doi.org/10.1016/j.ces.2014.09.046

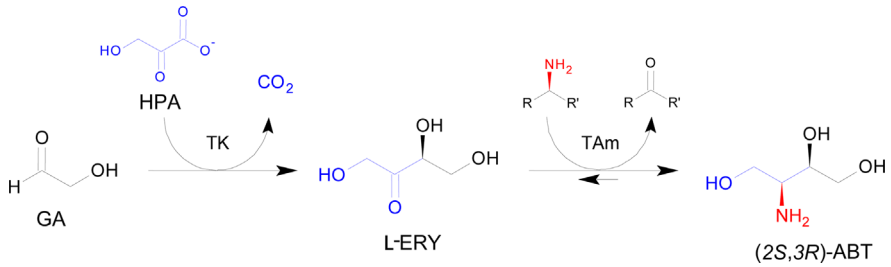

Scheme 1. Reaction scheme of the *de-novo* transketolase (TK)–transaminase (TAm) pathway for the synthesis of chiral amino-alcohol (2*S*,3*R*)-2-amino-1,3,4-butanetriol (ABT), from achiral substrates glycolaldehyde (GA) and hydroxypyruvate (HPA). TK intermediate product L-(+)-erythrulose (ERY). Amino-donor (*S*)-(−)-α-methylbenzylamine (MBA) R=Ph and R′=Me, isopropylamine (IPA) R=R′=Me.

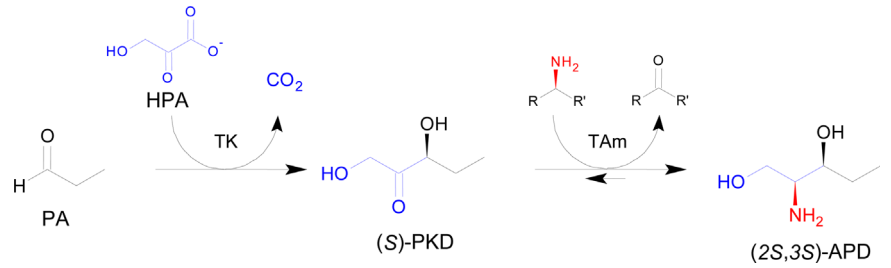

Scheme 2. Reaction scheme of the *de-novo* TK (D469E)-TAm pathway for the synthesis of chiral amino-alcohol (2*S*,3*S*)-2-aminopentane-1,3-diol (APD) from achiral substrates propionaldehyde (PA) and hydroxypyruvate (HPA). TK intermediate product is (3*S*)-1,3-dihydroxypentan-2-one (PKD). Amino-donor (*S*)-(−)-α-methylbenzylamine (MBA) R=Ph and R′=Me, isopropylamine (IPA) R=R′=Me.

novo pathways are ultimately applied *in vivo* (as a whole cell biocatalyst) or *in vitro* (as isolated or immobilised enzymes), there is a need to understand the mechanisms of the enzymes involved and to model reaction kinetics in order to optimise the overall conversion yield. This can be particularly challenging when designing synthetic routes involving engineered enzymes and when using non-natural reactants as frequently encountered in industrial syntheses (Meyer et al., 2007). In these cases appropriate reaction mechanisms must first be established and then kinetic parameters determined for multiple enzymes and a variety of potential starting reactants and pathway intermediates.

A particular target for *de novo* designed multi-step enzymatic conversions is the synthesis of complex chiral compounds from simple starting reactants (Roessner and Scott, 1996; Prather and Martin, 2008; Dalby et al., 2009). Ideally such reactants would be cheap, achiral and available from renewable sources (Keasling, 2010). Products such as chiral amino-alcohols are of considerable industrial interest and represent an important target for multi-step enzymatic syntheses. They are useful building blocks in the synthesis of a range of optically pure pharmaceuticals such as HIV protease inhibitors (Kaldor et al., 1997; Kwon and Ko, 2002), active molecules such as (*S*)-amphetamine (Rozwadoska, 1993) or broad spectrum antibiotics like chloramphenicol and thiamphenicol (Bhaskar, 2004).

Previously we have established a series of automated, microwell-based methods to inform early stage bioconversion process design and aid in quantitative prediction of larger scales process kinetics (Lye et al., 2003; Micheletti and Lye, 2006). We have also established 'mix and match' expression systems to rapidly trial pairs of enzymes for use in *de novo* engineered pathways. The utility of this approach was illustrated for a sequential, two-step synthesis comprising carbon-carbon bond formation using a transketolase (TK), followed by a transaminase (TAm) to create chiral amino-alcohols from achiral substrates (Rios-Solis et al., 2011). In that work the wild type *Escherichia coli* TK and the *Chomobacterium violaceum* 2025 (CV2025) TAm were selected for the one-pot synthesis of diastereoisomer (2*S*,3*R*)-2-amino-1,3,4-butanetriol (ABT) (Scheme 1), while the mutant *E. coli* TK D469E and the CV2025 TAm were selected for the synthesis of (2*S*,3*S*)-2-aminopentane-1,3-diol (APD) (Scheme 2). Nevertheless, the kinetic modelling and optimisation of multi-step biocatalytic processes has been poorly explored, due to the complexities of integrating the kinetic models for multiple enzymes and the number of kinetic parameters involved (Xue and Woodley, 2012). Improved modelling and simulation would enable hypothetical changes to be explored in *silico*, speeding up process development and allowing the evaluation of process control strategies, to ensure stability and the desired efficiency (Sin et al., 2009).

The aim of this work was to establish detailed kinetic models for each of the individual enzymatic reactions, exploiting our previously developed experimental methodologies, in order to optimise the overall conversion yields of ABT and APD (Schemes 1 and 2). Kinetic models for the various TK and TAm bioconversions were first obtained from microscale experimental data using previously established numerical techniques for rapid kinetic parameter determination (Chen et al., 2009; Rios-Solis et al., 2013). These combine traditional initial rate experiments, to identify a solution in the vicinity of the global minimum, with nonlinear regression methods to determine the exact location of the solution thus reducing the number of experiments required. Once established, the kinetic models were validated against preparative scale (50 mL) bioconversion data before being used to identify key reaction constraints (Pollard and Woodley, 2007) and simulate scenarios for optimal bioreactor operation. These were again verified experimentally illustrating the importance of kinetic modelling to underpin the design and optimisation of multi-enzymatic systems in synthetic biology.

2. Materials and methods

2.1. Materials

Molecular biology enzymes were obtained from New England Bio-laboratories (NEB, Hitchin, UK). Nutrient broth and nutrient agar were obtained from Fisher Scientific (Leicestershire, UK).

Competent *E. coli* BL21-Gold (DE3) cells were obtained from Stratagene (Amsterdam, NL). All other reagents were obtained from Sigma-Aldrich (Gillingham, UK) unless noted otherwise, and were of the highest purity available.

2.2. Synthesis of substrates and products

HPA was synthesised by reacting bromopyruvic acid with LiOH following a previously described method (Morris et al., 1996). PKD was synthesised in a 100 mL scale bioconversion with 300 mM HPA, 300 mM PA, 9 mM $MgCl_2$, 2.4 mM TPP, pH 7.0 and 30% v/v of D469E TK lysate (final TK concentration of 0.3 mg mL^{-1}). The reaction was stirred for 10 h at room temperature in a sealed flask and the pH was maintained at 7.0 using a 718 STAT Titrino pH controller (Metrohm Ion Analysis, Switzerland). The solution was dried on silica and purified by column chromatography (ethyl acetate: hexane, 1:1) to yield PKD as a colourless oil that crystallised on standing. ABT and APD product standards were prepared in a multi-step chemical synthesis described elsewhere (Ingram et al., 2007; Smith et al., 2010).

2.3. Plasmids

2.3.1. Transketolase plasmid and mutagenesis

Plasmid pQR412 contained the complete *E. coli* TK gene, *tktA*, with its native promoter and an N-terminal His6-tag. It was constructed using the expression vector pMMB67HE (8.8 kb), which has a RSF1010 origin of replication, the *tac* promoter, the Lac repressor and codes for resistance to ampicillin (Ingram et al., 2007). Even though the plasmid contained the inducible *tac* promoter, the expression of the *E. coli tktA* was constitutive because of the presence of its native promoter. Site direct mutagenesis on the TK gene was performed using the Quikchange kit (Stratagene, Amsterdan, NL) following the supplier's instructions. The primers used for the TK mutagenesis were the following:

D469E: TCGGTCTGGGCGAA**CAA**GGGCCGACTCACCAG

2.3.2. Transaminase plasmid

Plasmid pQR801 contained the complete *Chromobacterium violaceum* 2025 TAm gene with a His6-tag (GenBank accession no. NP_901695). Plasmid pQR801 was constructed using the expression vector pET29(a)+ (5.3 kb), which contains an inducible T7 promoter, the Lac repressor and codes for resistance to kanamycin (Kaulmann et al., 2007).

2.4. Biocatalyst preparation

2.4.1. Shake flask whole cell TK biocatalyst preparation

Competent *E. coli* BL21-Gold (DE3) cells were transformed with the plasmid pQR412 using the heat shock technique described by the supplier (Stratagene, Amsterdam, NL). An overnight culture of the transformed cells was obtained in a 100 mL shake flask (10 mL working volume) of LB-glycerol broth (10 g L^{-1} tryptone, 5 g L^{-1} yeast extract, 10 g L^{-1} NaCl and 10 g L^{-1} glycerol) containing 150 mg L^{-1} ampicillin. Growth was performed at 37 °C with orbital shaking at 250 rpm using an SI 50 orbital shaker (Stuart Scientific, Redhill, UK). The total volume of this culture was used to inoculate a 1 L shake flask (100 mL working volume) which was left to grow for 8 h. The cells were then harvested and following the removal of broth by centrifugation, they were resuspended in 200 mM HEPES buffer, pH 7.5 and used for whole cell bioconversions.

2.4.2. Shake flask whole cell TAm and TK–TAm biocatalyst preparation

Transformation of *E. coli* BL21-Gold (DE3) cells with the plasmid pQR801 and inoculum preparation were performed in the same way as the TK biocatalyst, except that 150 mg L^{-1} of kanamycin was used for the single transformed cells and 50 mg mL^{-1} of both kanamycin and ampicillin were used for the double transformed strain. After inoculation of a 1 L shake flask (100 mL working volume), when the OD_{600} reached a value of 1.5–2.0, isopropylthiogalactopyranoside (IPTG) was added to final concentration of 0.2 mM. After 4 h induction, the cells were harvested and following the removal of broth by centrifugation, they were resuspended in 200 mM HEPES buffer, pH 7.5 and used for whole cell bioconversions.

2.4.3. 5 L fermentations

Batch fermentations were carried out in a 7.5 L fermenter (BioFlo 110, New Brunswick, Hertfordshire, UK) with a working volume of 5 l. The baffled fermenter had an aspect ratio of 1.79:1 and Rushton impellers ($di/dt = 0.25$). The temperature was monitored by a thermocouple and automatically controlled at 30 or 37 °C via cold water circulation in the external jacket of the fermenter in addition to a heating jacket. The pH was measured by an Ingold gel filled pH probe (Ingold Messtechnik, Urdorf, Switzerland) and was controlled with the addition of 85% v/v H_3PO_4 (acid) and 28% NH_4OH v/v (base). DOT was monitored by a polarographic oxygen electrode (Ingold Messtechnik, Urdorf, Switzerland) and was maintained at 30% using control of the impeller speed and using gas blending with 100% oxygen when necessary. A solution of 80% polypropylene glycol was used as antifoam to control liquid levels using the automated antifoam probe. Ingoing air was sterilised by passage through a membrane filter and dispersed in the vessel at the base of the lower turbine with a ring sparger at a flow rate of 5 L min^{-1}.

The vessel was filled with 4.5 L LB glycerol media with a composition as described in Section 2.4.1 and all the probe calibrations and pre-sterilization procedures were performed following the manufacturer instructions. The fermenter was then sterilised as a complete unit in an autoclave at 121 °C for 20 min, and after the media was cooled down, filter-sterilised ampicillin and kanamycin were added to a final concentration of 150 mg L^{-1}. The fermenter was then inoculated aseptically with five 100 mL shake flasks cultures previously grown overnight. Data was logged by on-line measurements of DOT, pH, temperature and speed of the impeller using the BioCommand software (BioFlo 110, New Brunswick, Hertfordshire, UK) as well as by taking regular optical density measurements at 600 nm (OD_{600}) using a spectrophotometer (Thermo Spectronic, Cambridge, UK).

2.5. Bioconversion kinetics

2.5.1. Automated microscale experimental platform

Microscale bioconversions were performed in a glass 96-well, flat-bottomed microtiter plate with individual wells having a diameter of 7.6 mm and height of 12 mm (Radleys Discovery Technologies, Essex, UK). The microplate was covered with a thermo plastic elastomer cap designed to work with automated equipment (Micronic, Lelystad, Netherlands). All the bioconversions were performed using 300 μl total volume at 30 °C, pH 7.5 unless noted otherwise, and shaking was provided at 400 rpm with a Thermomixer Comfort shaker (shaking diameter of 6 mm, Eppendorf, Cambridge, UK) operated on the deck of a Tecan Genesis robotic platform (Tecan, Reading, UK). The concentration of TK cofactors $MgCl_2$ and thiamine pyrophosphate (TPP) were 9 mM and 2.4 mM respectively for all reactions. The

concentration of TAm cofactor pyridoxal-5-phosphate (PLP) was 0.2 mM in all cases. Previous studies have shown that initial incubation with cofactor was necessary to allow the enzymes to bind to PLP or TPP (Ellis and Davies, 1961; Van Ophem et al., 1998), therefore the whole cell suspension with the cofactor solutions were always added first in the well and left to incubate for 20 min at 30 °C, prior to initiation of the reaction with the addition of the substrate solutions. Aliquots of 20 µl were taken at various time intervals and quenched with 380 µl of a 0.1% v/v trifluoroacetic acid (TFA) solution. They were then centrifuged for 5 min at 5000 rpm and transferred into an HPLC vial for further analysis. All experiments were performed in triplicate. The specific activities were determined as the amount of PKD, ERY, acetophenone (AP), APD and ABT formed per unit of time normalised by the amount of enzyme used in the reaction.

2.5.2. Preparative scale bioconversions

Bioconversions at preparative scale (working volume of 50 mL) were performed in a 150 mL titration vessel with thermostat jacket (Metrohm Ion Analysis, Switzerland). Temperature was maintained at 30 °C using a circulating water bath (Grant Instruments, Cambridge, UK), mixing was achieved using a magnetic stirrer at 300 rpm, and the pH was maintained at pH 7.5 unless noted otherwise by the use of an automated addition of 1 M NaOH using a 718 STAT Titrino pH controller (Metrohm Ion Analysis, Switzerland). For preparative scale fed batch reactions, a peristaltic P-1 pump (Pharmacia Fine Chemicals, Uppsala, Sweden) was used to add the desired substrate solution over time.

2.6. Analytical methods

Biomass concentration was measured as optical density at 600 nm (OD_{600}) using a spectrophotometer (Thermo Spectronic, Cambridge, UK) and converted to dry cell weight (DCW) using a calibration curve where 1 $OD_{600}=0.4\ g_{DCW}\ L^{-1}$. Protein concentrations were obtained using Bradford assay and SDS-PAGE as described previously (Kaulmann et al., 2007). A Dionex HPLC system (Camberley, UK) with a Bio-Rad Aminex HPX-87H reverse phase column ($300\times 7.8\ mm^2$, Bio-Rad Labs., Richmond, CA, USA), controlled by Chromeleon client 6.60 software was used for the separation and analysis of PKD, ERY and HPA. The system comprised a GP50 gradient pump, a FAMOS autosampler, an LC30 chromatography column oven and an AD20 UV/vis absorbance detector and the method used has been described previously (Chen et al., 2009). To quantify MBA, AP, APD and ABT, an integrated Dionex Ultimate 3000 HPLC system (Camberley, UK) with an ACE 5 C18 reverse phase column (150 mm × 4.6 mm, 5 µm particle size; Advance Chromatography Technologies, Aberdeen, UK) controlled by Chromeleon client 6.60 software was employed and the method has been reported elsewhere (Kaulmann et al., 2007). To analyse ABT and APD, the samples were derivatized by addition of an excess of 6-aminoquinolyl-*N*-hydroxysuccinimidyl carbamate. The derivatizing reagent was made in house following a previously described protocol (Cohen and Michaud, 1993), and the HPLC method used has been described previously (Ingram et al., 2007). The enantiomeric excess (*ee*) of the ketodiols was determined by derivatization via dibenzoylation for satisfactory peak resolution by chiral HPLC, the method has been described in more detail elsewhere (Cázares et al., 2010). Examples of the different HPLC profiles have been published previously (Rios-Solis et al., 2011).

2.7. Nonlinear regresion methods

A programme was developed using Matlab® software (MathWorks, Natick, MA, USA) in order to automatically perform all the nonlinear regressions and statistical analyses following the routines for kinetic parameter estimation as previously described (Chen et al., 2008; Rios-Solis et al., 2013). All the nonlinear regressions were performed using the mesh adaptive pattern search algorithm in Matlab® known as: "The Genetic Algorithm and Direct Search Toolbox". This method was previously shown to be more likely to achieve global optimisation than gradient-based methods (Chen et al., 2008). All kinetic parameters are reported as apparent values given that all enzymes are used in the form of whole cell biocatalysts.

3. Results

3.1. Determination of enzyme kinetic parameters

In our previous work, several enzyme candidates and biocatalyst forms were evaluated for their specific activities, final yield and enantiomeric excess for the synthesis of amino-alcohols (Rios-Solis et al., 2011). The outcome was the construction of two whole cell biocatalysts; one comprising the *E. coli* wild type TK combined with the CV2025 TAm and the second comprising the mutant TK D469E combined with the CV2025 TAm for the synthesis of ABT and APD respectively (Schemes 1 and 2). The kinetic model and parameters for the TK synthesis of ERY from GA and HPA have been reported previously (Chen et al., 2009), likewise for the TAm mediated synthesis of ABT from ERY and MBA (Rios-Solis et al., 2013). In contrast the kinetic parameters for the TK D469E mediated synthesis of PKD and the subsequent CV2025 TAm mediated synthesis of APD were still unknown. Hence these kinetic parameters were determined here following the procedures described in our previous works (Chen et al., 2008; Rios-Solis et al., 2013).

3.1.1. TK kinetic models

Transketolase is an enzyme that catalyses carbon-carbon bond formation by transferring a C_2 moiety (1,2-dihydroxyethyl group) between a ketose sugar and an aldose sugar (Sprenger et al., 1995) The TK D469E catalysed synthesis of PKD from HPA and PA is an irreversible reaction due to the release of CO_2 as a side product (Scheme 2). The bioconversion follows a previously elucidated ping-pong bi–bi mechanism with competitive substrate inhibition, which requires thiamine pyrophosphate and Mg^{2+} as cofactors (Gyamerah and Willetts, 1997; Chen et al., 2008). The full kinetic model can thus be written as follows:

$$\frac{d[\mathrm{PKD}]}{dt}=\frac{k_{\mathrm{cat}}E_{i\mathrm{TK}}[\mathrm{HPA}][\mathrm{PA}]}{\mathrm{den}}$$

$$\mathrm{den}=K_{\mathrm{PA}}[\mathrm{HPA}]\left(1+\frac{[\mathrm{HPA}]}{K_{i\mathrm{HPA}}}\right)+K_{\mathrm{HPA}}[\mathrm{PA}]\left(1+\frac{\mathrm{PA}}{K_{i\mathrm{PA}}}\right)+[\mathrm{HPA}][\mathrm{PA}]+\frac{K_{\mathrm{HPA}}}{K_{i\mathrm{PKD}}}[\mathrm{PA}][\mathrm{PKD}]+\frac{K_{\mathrm{HPA}}K_{i\mathrm{PA}}}{K_{i\mathrm{PKD}}} \quad (1)$$

where k_{cat} represents the catalytic rate constant, K_{PA} and K_{HPA} are the Michaelis–Menten constants of PA and HPA, K_{iPA}, K_{iHPA} and K_{iPKD} are the inhibition constants of PA, HPA and PKD respectively, and E_{iTK} is the TK enzyme concentration. Note that the same kinetic model and equation applies for the synthesis of ERY, in which case the nomenclature for the keto-acceptor PA should be substituted by GA and product PKD by ERY.

Following the methodology described in our previous work (Chen et al., 2008), the values of the kinetic parameters were experimentally determined from microscale experimental data and are summarised in Table 1. Fig. 1 shows the experimental Michaelis–Menten plots for the synthesis of PKD, as well as two progress curves with microscale experimental data and model predictions. The reliability and adequacy of the kinetic

determination methodologies used in this work, as well as the validation of the TK model using GA have been performed elsewhere (Sayar et al., 2009a, 2009b). In that work, among the six kinetic parameters of the TK model, only 3 were found to display a positive effect on the performance of the reaction (positive sensitivity), which were the Michaelis–Menten constant for GA (K_{GA}), inhibition constant for HPA (K_{iHPA}), and the catalytic rate constant k_{cat}. Excellent agreement was found between the experimental and predicted values (Fig. 1c and d). The apparent k_{cat} for the synthesis of PKD using TK mutant D469E was found to be similar to the previously published value using *E. coli* TK mutant D469T in lysate form (Chen et al., 2008). Interestingly, both Michaelis–Menten constants found in this work were half the value than the ones published for TK D469T. Although non-hydroxylated aliphatic aldehydes can be accepted by TK, the activity is typically very low (Cázares et al., 2010; Smith et al., 2010). The variant TK D469E was engineered to work towards non-hydroxylated aliphatic aldehydes like PA; the result of a k_{cat} value of 642 min^{-1} is impressive, although it is still 5 times smaller than the wild type enzyme using hydroxylated aldehyde GA (Chen et al., 2009). The inhibition constants were found to be all in the same order of magnitude (Table 1). The enantiomeric excess of PKD was determined to be ~90%, which was in agreement with previous works (Cázares et al., 2010, Rios-Solis et al., 2011).

Table 1
Experimentally established values of the apparent kinetic parameters in Eq. (1) for the *E. coli* TK D469E mediated synthesis of PKD and the wild type *E. coli* TK mediated synthesis of ERY. The values of the parameters for the synthesis of PKD were determined according to the methodology of Chen et al. (2008) using a whole biocatalyst at pH 7.5 and 30 °C. The values of the parameters for the synthesis of ERY were obtained from literature (Chen et al., 2009).

Apparent kinetic parameter	Synthesis of PKD keto-acceptor: PA	Synthesis of ERY keto-acceptor: GA
Rate constant: k_{cat} (min^{-1})	642	2442
Michaelis constant for HPA: K_{HPA} (mM)	5	18
Michaelis constant for keto-acceptor: K_{PA} or K_{GA} (mM)	47	16
Inhibition constant for HPA: K_{iHPA} (mM)	87	40
Inhibition constant for keto-acceptor: K_{iPA} or K_{iGA} (mM)	542	570
Inhibition constant for ketodiol: K_{iPKD} or K_{iERY} (mM)	887	536

3.1.2. TAm kinetic models

TAm catalyses enzymatic amino group transfer by a ping-pong bi–bi mechanism and requires the cofactor pyridoxal 5′-phosphate to catalyse the reaction (Bulos and Handler, 1965; Kuramitsu et al., 1990). The reaction mechanism is composed of two half reactions, where in the first half reaction, the amino-donor binds to the enzyme and the amino group is transferred to the pyridoxal 5′phosphate cofactor, which forms pyridoxamine 5-phosphate

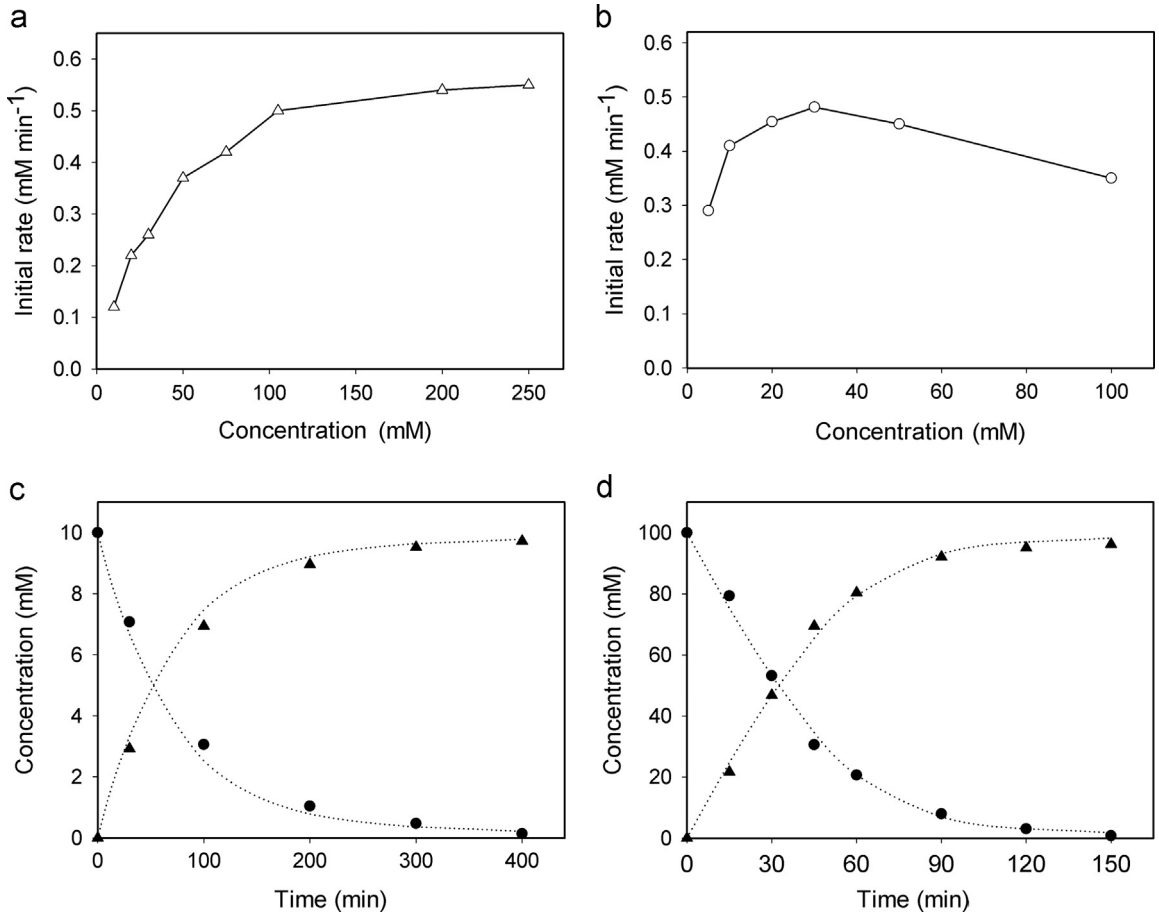

Fig. 1. (a) Microscale kinetic data showing apparent initial rate of PKD synthesis using TK D469E as a function of [PA] while maintaining [HPA] fixed at 30 mM, and (b) as a function of [HPA] while maintaining [PA] fixed at 100 mM. For the experiments (a) and (b) [TK] concentration was 0.15 mg mL^{-1}. Experiments (c) and (d) represent typical experimental progress curves and model fits using initial concentrations of (c) 10 mM [PA] and [HPA] and 0.1 mg mL^{-1} [TK] and (d) 100 mM [PA] and [HPA] and 0.4 mg mL^{-1} [TK] showing (•) HPA utilisation and (▲) PKD production. Dotted lines show model predictions based on Eq. (1) using the final kinetic parameters in Table 1. For all the experiments TK biocatalyst was used in whole cell form with 2.4 mM [TPP] and 9 mM [Mg^{2+}] at 30 °C and pH 7.5 in 200 mM HEPES buffer.

(PMP), and the respective keto product is released. During the second half reaction, PMP (bounded to TAm) transfers the amino group to the acceptor substrate and PLP is regenerated, while the new aminated compound is released (Bulos and Handler, 1965).

It has been reported that in some TAm bioconversions substrate or product can bind an incorrect enzyme-cofactor form, creating dead end complexes that cannot react further, causing a potentially strong form of inhibition (Bulos and Handler, 1965; Shin and Kim, 1998, 2002). For the CV2025 TAm mediated synthesis of APD, the presence of abortive complexes has not previously been shown. Therefore, a recently developed routine was experimentally applied to the TAm mediated synthesis of APD to elucidate the partially unknown reaction mechanism and the values of its parameters (Rios-Solis et al., 2013). Substrate inhibition was found by the formation of the dead end complex E–PMP–MBA,

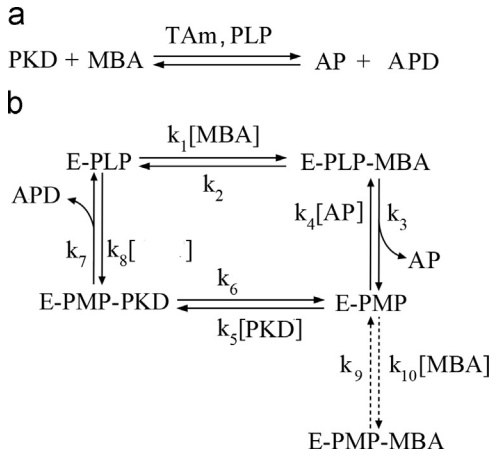

Fig. 2. Proposed reaction mechanism for the TAm mediated synthesis of APD. Solid lines represent the basic kinetic model without the formation of abortive complexes. Dashed arrows represent substrate inhibition via formation of dead end complex E–PMP–MBA. The reaction mechanism was selected based on the systematic routine described in Rios-Solis et al. (2013).

which was in agreement with the form of inhibition exhibited in the TAm mediated synthesis of ABT using MBA as amino-donor (Rios-Solis et al., 2013). The reaction mechanism is shown in Fig. 2 and the corresponding mathematical model is given in the following equation

$$v = \frac{k_f k_r E_{iTAm}([MBA][PKD] - ([AP][APD]/K_{eq}))}{den}$$

$$den = k_r K_{MBA}[PKD] + k_r K_{PKD}[MBA] + k_r[PKD][MBA] + \frac{k_f K_{AP}[APD]}{K_{eq}} + \frac{k_f K_{APD}[AP]}{K_{eq}} + \frac{k_f[AP][APD]}{K_{eq}} + \frac{k_r K_{MBA}[PKD][APD]}{K_{iAPD}} + \frac{k_f K_{APD}[MBA][AP]}{K_{eq} K_{iMBA}} \quad (2)$$

where k_f and k_r represents the catalytic rate constants for the forward and reverse reaction respectively, K_{PKD}, K_{AP}, K_{APD} and K_{MBA} are the Michaelis–Menten constants of PKD, AP, APD and MBA, K_{iAPD} and K_{iMBA} are the inhibition constants of APD and MBA respectively, E_{iTAm} represents the TAm concentration and K_{eq} is the equilibrium constant. Again, it should be noted that the same kinetic model applies for the synthesis of ABT, and in the nomenclature the amino-acceptor PKD should be substituted by ERY and product APD by ABT. As for TK, the kinetic parameters were determined and are summarised in Table 2.

Fig. 3 shows the experimental Michaelis–Menten plots determined for both the forward and reverse reactions. The figure also shows two progress curves comparing microscale experimental data and model predictions for different initial substrate concentrations. Good agreement was again found between the experimental and predicted data (Fig. 3). A more detailed discussion about the uncertainty and validation of the kinetic parameters has been performed previously for the TAm mediated synthesis of ABT (Rios-Solis et al., 2013). In that work, a sensitivity analysis suggested a crucial bottleneck was the second half reaction of the ping pong bi–bi mechanism, in part due to the high Michaelis Menten constant of substrate ERY. The apparent forward catalytic

Table 2
Experimentally established values of the apparent kinetic parameters for Eq. (2) for the synthesis of APD catalysed by a whole cell *E. coli* biocatalyst containing the CV2025 TAm. The parameters for APD synthesis were obtained experimentally following our previously described methodology and the parameters for ABT synthesis were obtained from literature (Rios-Solis et al., 2013).

Kinetic parameter	Kinetic parameter in terms of rate constants	Synthesis of APD Substrate: PKD	Synthesis of ABT Substrate: ERY
(1) Catalytic rate constants (min^{-1})			
Rate constant forward reaction: k_f	$\frac{k_3 k_7}{k_3 + k_7}$	37	95
Rate constant reverse reaction: k_r	$\frac{k_2 k_6}{k_2 + k_6}$	1.9	12
(2) Michaelis–Menten constants (mM)			
Michaelis constant for MBA: K_{MBA}	$\frac{k_7(k_2 + k_3)}{k_1(k_3 + k_7)}$	1.2	0.5
Amino-acceptor Michaelis constant: K_{ERY} or K_{PKD}	$\frac{k_3(k_6 + k_7)}{k_5(k_3 + k_7)}$	20	95
Michaelis constant for AP: K_{AP}	$\frac{k_6(k_2 + k_3)}{k_4(k_2 + k_6)}$	18	16
Amino-alcohol Michaelis constant: K_{ABT} or K_{APD}	$\frac{k_2(k_6 + k_7)}{k_8(k_2 + k_6)}$	23	37
(3) Inhibition constants (mM)			
Inhibition constant for MBA: K_{iMBA}	$\frac{k_2}{k_1}$	5.0×10^{-3}	4.0×10^{-3}
Amino-acceptor inhibition constant: K_{iERY} or K_{iPKD}	$\frac{k_6}{k_5}$	0.2	1.0
Inhibition constant for AP: K_{iAP}	$\frac{k_3}{k_4}$	1.4	1.1
Amino-alcohol inhibition constant: K_{iABT} or K_{iAPD}	$\frac{k_7}{k_8}$	5.3	3.1
Inhibition constant for MBA complex: K_{iMBAc}	$\frac{k_9}{k_{10}}$	26	24
(4) Equilibrium constants			
Global equilibrium constant: K_{eq}	$\frac{k_1 k_3 k_5 k_7}{k_2 k_4 k_6 k_8}$	6407	843
Equilibrium constant for the first half reaction: K_1	$\frac{k_1 k_5}{k_2 k_4}$	280	275
Equilibrium constant for the second half reaction: K_2	$\frac{k_5 k_7}{k_6 k_8}$	22	3.1

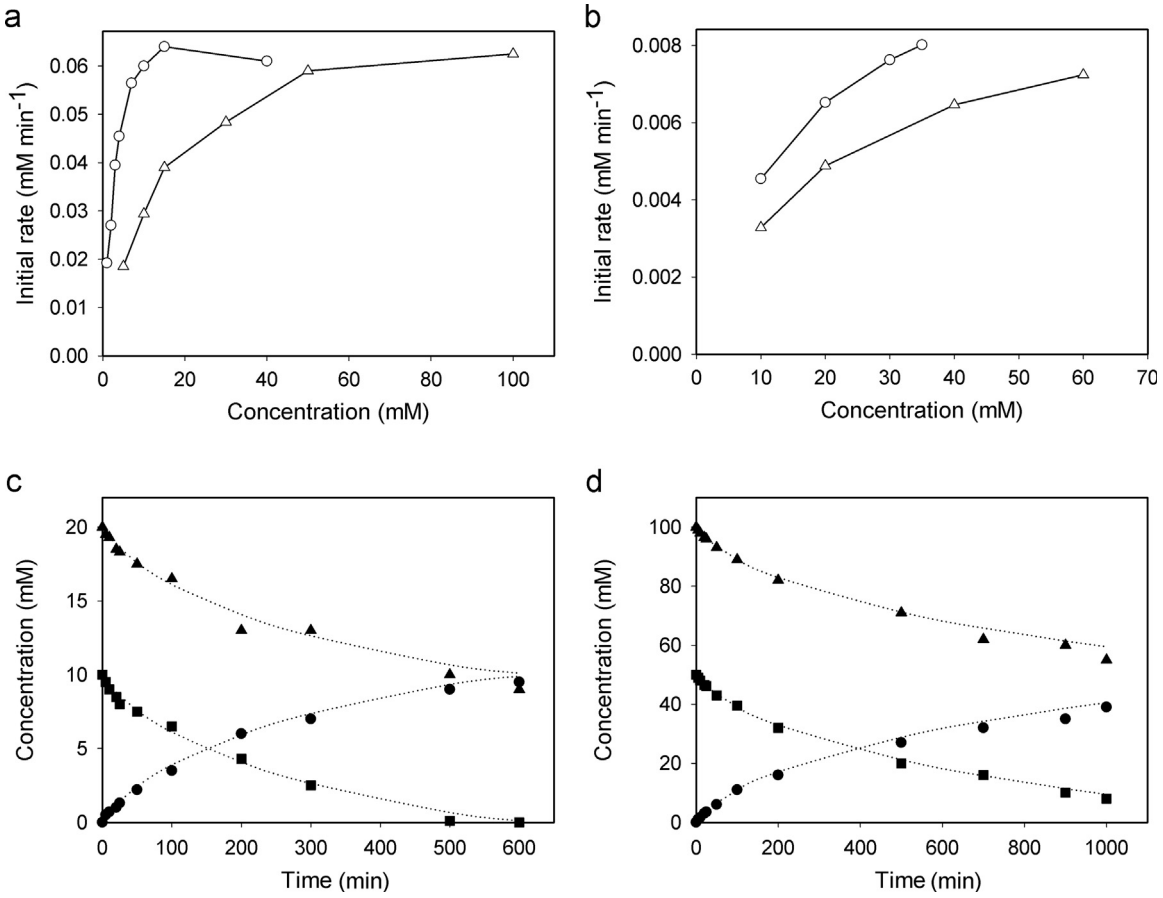

Fig. 3. (a) Microscale kinetic data showing apparent initial rate of AP formation for the forward reaction as a function of (○) [MBA] while maintaining [PKD] fixed at 100 mM, and as a function of (Δ) [PKD] while maintaining [MBA] fixed at 10 mM. (b) Apparent initial rate of MBA formation for the TAm reverse reaction as a function of (○) [AP] while maintaining [APD] fixed at 100 mM, and as a function of (Δ) [APD] while maintaining [AP] fixed at 35 mM. For experiments (a) and (b) [TAm] concentration was 0.3 mg mL^{-1}. Experiments (c) and (d) represent typical experimental TAm progress curves and model predictions using an initial concentration of (c) 20 mM [PKD] and 10 mM [MBA] and 0.2 mg mL^{-1} [TAm] and (b) 100 mM [PKD] and 50 mM [MBA] and 0.3 mg mL^{-1} [TAm] following(▲) PKD, (■) MBA and (●) APD. Dotted lines show model predictions based on Eq. (2) and final kinetic parameters in Table 2. For all the experiments TAm biocatalyst was used in whole cell form with 0.2 mM [PLP] at 30 °C and pH 7.5 in 200 mM HEPES buffer.

rate constant for the TAm mediated synthesis of PKD was 3-fold smaller than the one reported for the synthesis of ERY (Rios-Solis et al., 2013). In contrast, the Michaelis–Menten constant of PKD was 5 times smaller than the one determined for ABT synthesis, while the rest of the constants were in the same order of magnitude (Table 2). Simulations showed that by using the same enzyme concentration, the conversion rate of ERY by TAm to ABT would be relatively faster than the one of PKD to APD at concentrations above 200 mM. Nevertheless, at concentration below 30 mM, the low Michaelis–Menten constant of PKD compared to ERY would compensate the higher catalytic constant for ERY, giving comparable reaction rates for both amino-acceptors (simulation not shown).

3.2. *Production of dual TK–TAm biocatalyst for the one-pot syntheses*

When performing a multi-step biosynthesis, the choice of using pure enzymes or whole cells is fundamental to the design of the process. Using isolated enzymes involves higher upstream costs while whole-cell processes demands additional downstream costs (Woodley, 2006). In the case of TAm, it was found to have better catalytic efficiencies in the whole cell form due to increased enzyme stability (Halim et al., 2014; Rios-Solis et al., 2013). Although both TK and TAm biocatalysts could be added independently, so as to match their kinetic activities, this would double the cost of biocatalyst production. Furthermore, as progress is made to include larger numbers of enzymes in designed synthetic pathways then the efficiency of expression in a single host, with matched expression levels, will be critical for industrial implementation. The “mix and match” expression system, first proposed Hussain and Ward (2003), would facilitate the necessary separate regulation of TK and TAm expression in *E. coli* being based on two plasmids with different origins of replication and antibiotic resistance genes (Rios-Solis et al., 2011).

Based on the above results, the k_{cat} of TK was 17 or 25 times higher than the corresponding TAm k_{cat} values in the *de novo* pathways to synthesise APD and ABT respectively (Tables 1 and 2). The optimum enzyme ratio would also depend on the concentration of the different substrates used but assuming an equimolar substrate ratio, due to the reaction stoichiometry, simulations showed the most effective TAm/TK ratio would be 19 and 12 for the ABT and APD one pot syntheses respectively.

In this work it was found that by manipulating the fermentation temperature and induction time, it was possible to modify the final TK and TAm concentration of the enzymes in the whole cell biocatalyst. Fig. 4 shows the expression profiles of TK and TAm during a 5 L fermentation at 30 and 37 °C with early and late exponential phase induction of TAm with IPTG (0.1 mM). It was found that by performing the 5 L fermentation at 37 °C with early exponential phase induction of TAm, it was possible to achieve a final biomass concentration of $8.5 \pm 0.5\ g_{DCW}\ L^{-1}$ after 8 h of fermentation (specific growth rate of $0.43 \pm 0.07\ h^{-1}$). The final

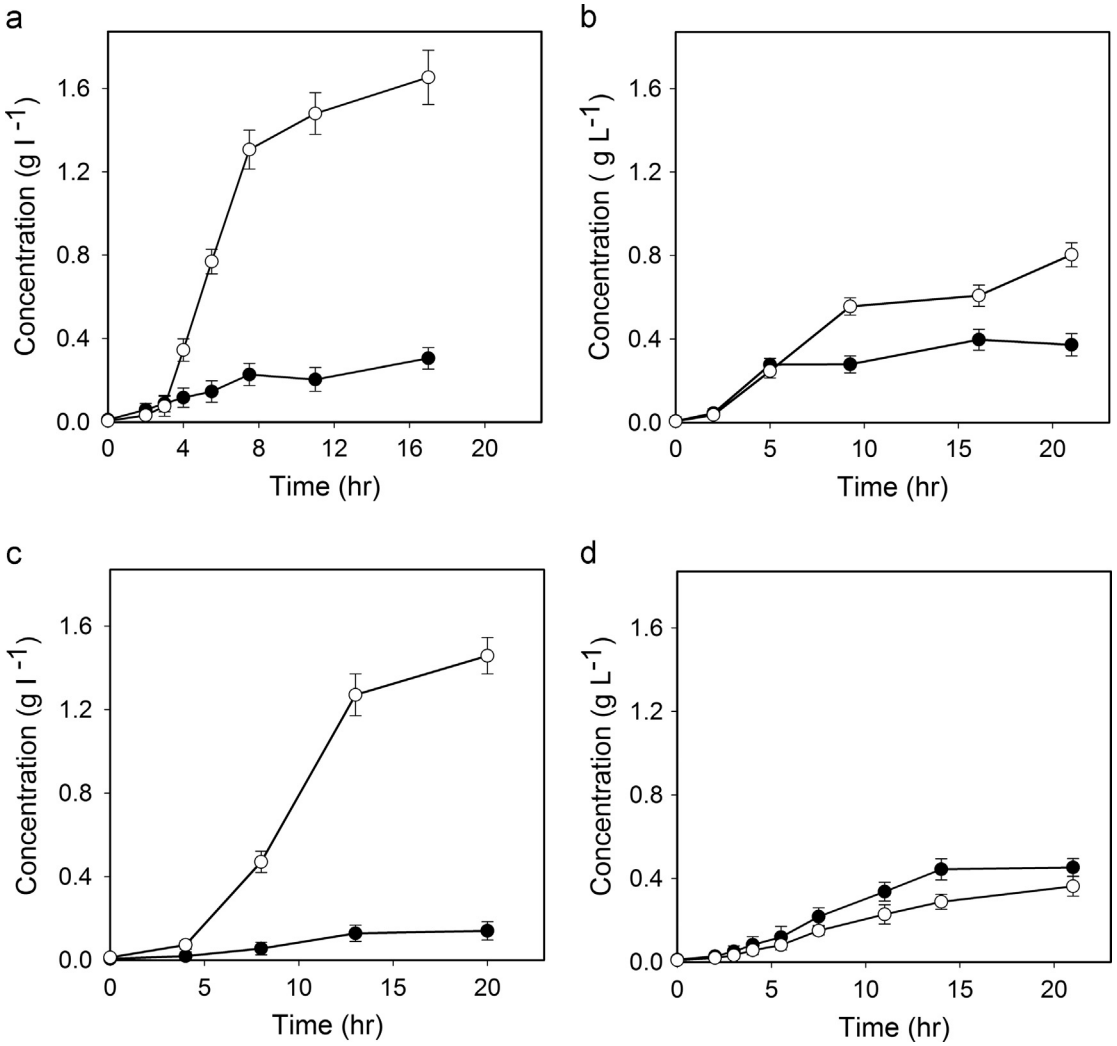

Fig. 4. Concentration profiles of wild type TK (•) and TAm (○) in a 5 L fermentation performed at 37 °C with 0.1 mM IPTG induction in the (a) early and (b) late exponential growth phase and at 30 °C with induction in the early (c) and (d) late exponential phase. The concentration of each enzyme was calculated assuming that 50% of the total dry cell biomass of *E. coli* cells were proteins (Watson, 1972), and by obtaining the percentage of total protein of the corresponding enzyme by SDS-PAGE. Error bars represent one standard deviation about the mean ($n=3$).

Table 3
Comparison of the different bioreactors and reaction conditions used for operation of the multi-step syntheses using the two dual TK–TAm whole cell *E. coli* biocatalysts.

Bioconversion scale	Microscale	Preparative scale
Temperature (°C)	30	30
Mixing device	Orbital shaking platform (diameter=6 mm)	Magnetic stirrer
Mixing (rpm)	300	300
Working reaction volume	300 μl	50 mL
Reactor vessel	550 μl micro reactors (96 well glass microplate)	150 glass stirred bioreactor
pH	7.5	7.5
pH control	200 mM HEPES buffer	pH-stat using 1 M NaOH (aq)

TAm and wild type TK concentrations were of 1.7 ± 0.1 and 0.31 ± 0.05 g L^{-1} (Fig. 4a), representing 39% and 7% respectively of the total cellular protein as determined by SDS PAGE (TAm/TK ratio of 6). Similar results were obtained for the dual TK D469E and the CV2025 TAm whole cell biocatalyst. This enzyme ratio was 2 and 3 times smaller than the optimum value determined for the synthesis of APD and ABT respectively.

A fermentation performed at 30 °C with early induction achieved the highest TAm/TK ratio of 9 compared to the value of 6 obtained with the corresponding fermentation at 37 °C. However, the high ratio at 30 °C was achieved due to a 43% decrease in TK expression compared to the result at 37 °C. This was not desirable for the one pot synthesis of amino alcohols, where a higher TAm/TK ratio is favourable. Overall, not only was the TK expression higher at 37 °C with early induction, but also the TAm expression was higher, making the biocatalyst produced at 37 °C with early induction economically more suitable for the multi-step synthesis of amino alcohols. These two dual TK–TAm whole cell biocatalysts were subsequently used for one-pot bioconversions at both microwell and preparative scales.

3.2.1. Comparison of micro- and preparative scale one-pot bioconversion kinetics

After the individual kinetic models of all the enzymes were obtained, the one-pot syntheses of ABT and APD (Schemes 1 and 2) were experimentally performed in 300 μl parallel microwell bioconversions and in 50 mL working volume preparative scale bioconversions. This represented a 167-fold scale translation over which the previously established kinetic models could be validated. Table 3 compares the different conditions and bioreactor formats used. The main difference between the two scales of operation was that the pH of the preparative scale bioconversion was maintained at 7.5 by the use of automated pH-stat addition of 1 M NaOH in comparison to use of 200 mM HEPES buffer in the microscale system (Table 3).

3.2.2. Modelling and scale-up of the one-pot synthesis of APD

Previous work has identified that the TAm amino-donor MBA could cause a side reaction when bioconversions were operated in a one-pot mode involving transfer of an amino group to the TK substrate HPA to yield serine (Rios-Solis et al., 2011). To overcome this issue, MBA was subsequently added in a single fed-batch addition after the TK reaction was completed. For the one-pot synthesis of APD, the final whole cell biomass concentration used was 2.1 $g_{DCW}\,L^{-1}$, with TAm and TK concentrations of 0.4 and 0.07 mg mL^{-1} respectively. The initial concentration of substrates PA and HPA were 10 mM, and using Eq. (1) it was predicted that the TK reaction would reach completion after 7 h, which was the time when TAm amino-donor MBA was added. A stock solution of 300 mM of the amino-donor was used, therefore the volume added of the MBA solution represented only 3% of the original reaction volume, and consequently the dilution of substrates and products was considered negligible. Fig. 5 shows the experimental progress curves of the micro and preparative scale multi-step synthesis of APD. Combining Eqs. (1) and (2), the complete modelling of the one-pot synthesis was also achieved. The microscale bioconversion kinetics generally show very good agreement with those from the preparative scale synthesis. A summary of the experimental kinetics and yields at the different scales and those from the model predictions is provided in Table 4.

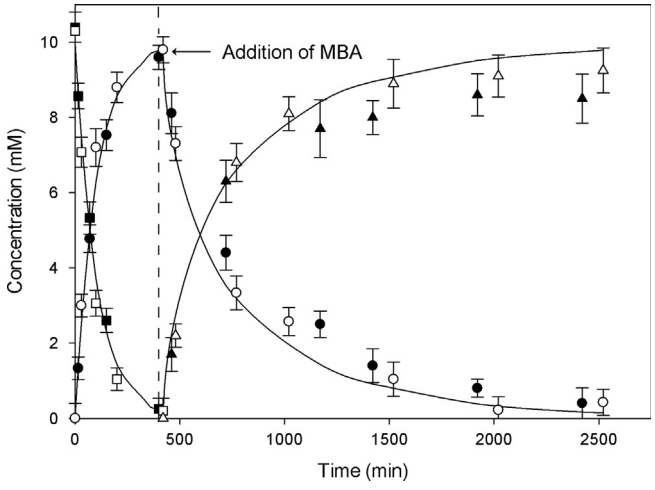

Fig. 5. Scale-up and modelling of the whole cell *E. coli* TK–TAm one-pot synthesis of APD following: (□) HPA, (○) PKD and (△) APD using microscale experimentation and (■) HPA, (●) PKD and (▲) APD for the preparative scale synthesis. Reaction conditions: 10 mM [HPA] and [PA], 0.2 mM [PLP], 2.4 mM [TPP], 9 mM [Mg^{2+}], 30 °C, pH 7.5. 10 mM MBA was added after 420 min. [TK] and [TAm] were 0.07 and 0.4 mg mL^{-1} respectively in whole cell form. Kinetic profiles (solid lines) modelled by combining Eqs. (1) and (2) with the corresponding kinetic parameters from Tables 1 and 2. Error bars represent one standard deviation about the mean ($n=3$).

The difference in TK and TAm specific activities of both scales were statistically not significant (Table 4). This indicates that the biocatalyst did not lose activity in the scale-up process, and also that the preparative scale synthesis did not suffer any mass transfer limitations. Excellent agreement was found between the predicted specific activities and the experimental data, which shows that the mathematical models developed using microscale data were still valid for preparative scale multi-step syntheses. After 1500 min of bioconversion, a small difference could be observed between the predicted and experimental data, which was higher than the experimental error, especially for the preparative scale synthesis. This discrepancy could also be detected in the final yield (% mol/mol) of the large scale bioconversion which was 7 and 13% smaller than the predicted and microscale data respectively. Because the predicted initial specific activities were in agreement with the experimental results of both scales (Table 4), and the discrepancies only appeared after 1500 min of reaction, the difference in the final conversion was attributed to a decrease in stability of TAm, probably caused by the toxicity of MBA. Toxicity of the amino-donor towards TAm has also been reported in other works (Yun et al., 2004; Rios-Solis et al., 2013). In addition, although APD was a non-natural substrate, consumption of APD by the whole cells could also contribute to the difference in yields, as it has previously been shown for similar amino-alcohols (Ingram et al., 2007). Others who have investigated scale-up of TAm bioconversion from the μl to mL scale have reported a 30% difference in the final yield (% mol/mol) mainly attributed to pH fluctuations in the small scale system (Truppo et al., 2009). The use of 200 mM HEPES here enabled the maintenance of a constant pH thus helping to improve agreement between the different scales.

3.3. Modelling and scale-up of the one-pot synthesis of ABT

In the same way as for the one-pot synthesis of APD, the one-pot synthesis of ABT (Scheme 1) was performed at the two scales. Due to the higher susceptibility of ERY and ABT to be consumed by side reactions in whole cell systems compared to PKD and APD (Ingram et al., 2007), 25% less biomass concentration was used. Therefore the concentration of TK and TAm were 0.05 and 0.3 mg mL^{-1} and the starting concentration of substrates GA and HPA was 30 mM. Eq. (2) predicted that after 250 min, the TK bioconversion would reach completion. After this time, MBA was added to a final concentration of 10 mM in the same way as for the synthesis of APD. An excess of ERY to MBA of 3:1 was maintained in the bioconversion due to the lower TAm Michaelis–Menten constant for ERY compared to MBA (Table 2). This was done with the aim to speed-up the one-pot synthesis and avoids enzyme

Table 4
Experimental reaction rates and yields for the one-pot synthesis of APD shown in Fig. 5 based on microscale and preparative scale bioreactor data. The predicted values were obtained using Eqs. (1) and (2) with the kinetic parameters from Tables 1 and 2 respectively.

Apparent kinetic parameter	Microscale data	Preparative scale data	Model prediction
E. coli D469E TK initial specific activity (μmol min^{-1} mg^{-1})	1.3 ± 0.2	1.2 ± 0.2	1.1
CV2025 TAm initial specific activity (μmol min^{-1} mg^{-1})	0.1 ± 0.01	0.1 ± 0.02	0.12
Final APD yield (% mol/mol)	93 ± 6	85 ± 6.5	98

deactivation by MBA, as well as ABT and ERY consumption by the whole cells.

Fig. 6 shows the complete experimental progress curves of the micro and preparative scale bioconversions. Combining Eqs. (1) and (2) with their respective parameters (Tables 1 and 2) again enabled modelling of the complete conversion profile. Good agreement was found between the two scales with a maximum experimental difference in ABT synthesis of 11%, which was not statistically significant. The kinetic results from the different scales and the model are summarised in Table 5.

For this second bioconversion there was a 25% difference between the TK experimental and predicted specific activity (Table 5). This was probably because the TK kinetic model used from literature was established at 25 °C and pH 7.0 (Chen et al., 2009), instead of 30 °C and pH 7.5 as used here. The difference was considered acceptable however, and good agreement could be concluded between the predicted and experimental data, validating the microscale mathematical models for preparative scale multi-step synthesis. As with the one-pot synthesis of APD, the ABT yield (% mol/mol) of the preparative scale conversion was 10 and 15% smaller than the microscale and predicted data (Table 5). Also some consumption of ERY by the whole cell was observed in both scales (Fig. 6). Nevertheless, by using an excess of 3:1 ERY: MBA, the reaction time to reach completion was reduced by 3 fold compared to an equimolar concentration of 10 mM (Eq. (1) and Table 1). The reduction in time allowed less consumption of ABT and ERY by the whole cells, as well as less inactivation of TAm by MBA.

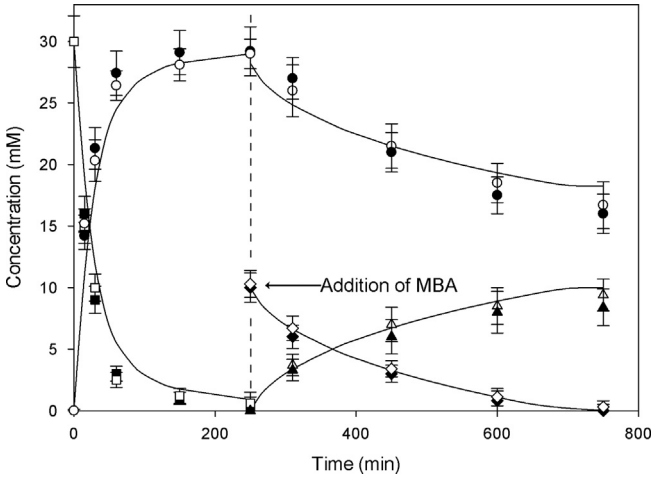

Fig. 6. Scale-up and modelling of the whole cell *E. coli* TK–TAm one-pot synthesis of ABT following: (□) HPA, (○) ERY and (△) ABT using microscale experimentation, and (■) HPA, (●) ERY and (▲) ABT for the preparative scale synthesis. Reaction conditions: 30 mM [HPA] and [PA], 0.2 mM [PLP], 2.4 mM [TPP], 9 mM [Mg^{2+}], 30 °C, pH 7.5. MBA was added to a concentration of 10 mM after 250 min. [TK] and [TAm] were 0.05 and 0.3 mg mL^{-1} in whole cell form. Kinetic profiles (solid lines) modelled by combining Eqs. (1) and (2) with the corresponding kinetic parameters from Tables 1 and 2. Error bars represent one standard deviation about the mean ($n=3$).

3.4. Selection of optimum reactor operating conditions

3.4.1. One-pot synthesis of ABT with fed-batch addition of MBA

Following validation of the bioconversion models, they were used to select the best reactor operating conditions to further increase the bioconversion yields. MBA was found to be inhibitory to TAm, which is in agreement with previous studies where problems with TAm were encountered at concentrations greater than 10 mM (Rios-Solis et al., 2013). This limited the yield of the TAm bioconversion in equimolar concentrations above 10 mM. A solution to avoid MBA toxicity and inhibition is to use continuous fed-batch addition of the amino-donor. The Michaelis–Menten constant of ERY was found in previous work to be 97 mM in comparison with the one for MBA of 0.5 mM (Rios-Solis et al., 2013). These values predicted that the production rate of ABT would not be severely affected by maintaining an MBA concentration below 10 mM in the bioconversion.

Consequently, a one-pot synthesis of ABT was performed at preparative scale with fed-batch addition of MBA. The initial volume of the bioconversion was 50 mL, and the pH and temperature were controlled at 7.5 and 30 °C. The initial concentration of HPA and GA was 100 mM which was 10 fold higher than in Fig. 5. The concentration of TK and TAm were 0.75 and 0.14 mg mL^{-1} respectively using a whole cell biocatalyst. To model the one-pot synthesis with fed-batch addition of MBA, Eqs. (1) and (2) were combined with the following differential equations to model the TAm step:

$$\frac{d[\mathrm{MBA}]}{dt} = -R_{\mathrm{MBA}} + \frac{\mathrm{FeedRate} \times \mathrm{MBAFeed}}{\mathrm{Vol}} - \frac{[\mathrm{MBA}] \times \mathrm{FeedRate}}{\mathrm{Vol}} \quad (3)$$

$$\frac{d[\mathrm{ERY}]}{dt} = -R_{\mathrm{ERY}} - \frac{[\mathrm{ERY}] \times \mathrm{FeedRate}}{\mathrm{Vol}} \quad (4)$$

$$\frac{d[\mathrm{ABT}]}{dt} = R_{\mathrm{ABT}} - \frac{[\mathrm{ABT}] \times \mathrm{FeedRate}}{\mathrm{Vol}} \quad (5)$$

$$\frac{d\mathrm{Vol}}{dt} = \mathrm{FeedRate} \quad (6)$$

where R_i (mM min^{-1}) is the kinetic reaction rate of each compound defined by Eq. (2), FeedRate (l min^{-1}) is the rate of MBA solution added, MBAFeed (mM) is the concentration of MBA in the feed and Vol (l) is the working reaction volume.

Eq. (1) predicted that under the previously mentioned conditions, the TK reaction would reach completion after 180 min, at this time MBA was fed continuously as a 300 mM solution. A variable flow rate of the MBA solution that would match the predicted rate of the consumption of the amino-donor by Eq. (3) would have been desirable (Sayar et al., 2009a, 2009b), however this can be difficult to achieve in practice. Several simulations were thus performed using Eqs. (3)–(6) to identify an appropriate constant flow rate, which would maximise the reaction rate while maintaining a concentration of MBA < 10 mM for the maximum possible time. The selected flow rate was 0.31 mL h^{-1}, which combined with a calculated duration of the fed-batch operation of 53 h, meant that a total of 5 mmol of MBA would be added to the reaction equivalent to a normalised concentration of 100 mM for an initial reaction volume of 50 mL.

Table 5
Experimental reaction rates and yields for the one-pot synthesis of ABT shown in Fig. 6 based on microscale and preparative scale bioreactor data. The predicted values were obtained using Eqs. (1) and (2) with the kinetic parameters from Tables 1 and 2 respectively.

Apparent kinetic parameter	Microscale	Preparative scale	Predicted data
Wild type TK initial specific activity (μmol min^{-1} mg^{-1})	2.0 ± 0.2	1.9 ± 0.2	1.5
CV2025 TAm initial specific activity (μmol min^{-1} mg^{-1})	0.21 ± 0.02	0.18 ± 0.02	0.19
Final ABT conversion (% mol/mol)	94 ± 9	84 ± 11	99

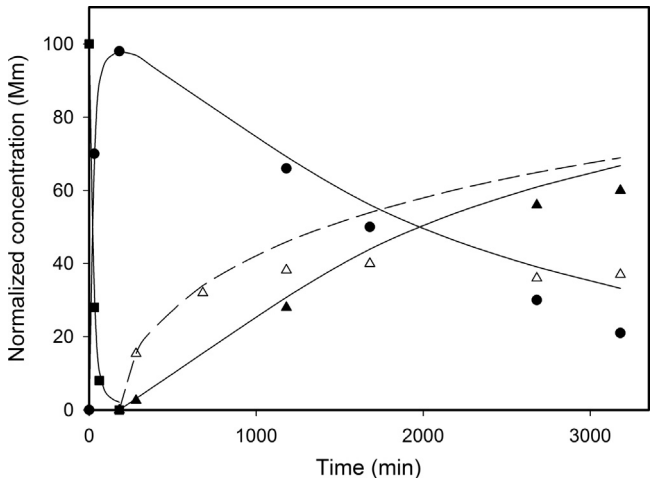

Fig. 7. Typical progress curves for modelling the TK–TAm one-pot synthesis of ABT with continuous fed-batch addition of MBA (reference volume of 50 mL): (■) HPA, (●) ERY and (▲) ABT, and with a single shot addition of MBA showing (△) ABT for preparative scale bioconversions. Initial reaction conditions: 50 mL working volume, 100 mM [HPA] and [GA], 0.2 mM [PLP], 2.4 mM [TPP], 9 mM [Mg^{2+}], 30 °C, pH 7.5, 25 mM HEPES. For the fed-batch addition, a solution of 300 mM [MBA] was added after 180 min with a constant flow rate of 0.31 mL h^{-1} or 5 mmol of pure MBA was added in the single shot addition of the amino-donor. [TK] and [TAm] were 0.14 and 0.75 mg mL^{-1} respectively in whole cell form. Kinetic profiles modelled by combining Eqs. (2)–(6) with the corresponding kinetic parameters from Tables 1 and 2 for continuous fed-batch (solid lines) and single shot (dashed line) addition of MBA.

Fig. 7 shows the experimental progress curves and the predicted normalised concentration for the one-pot synthesis of ABT with fed-batch MBA addition. In order to compare the performance of the different MBA addition modes, another one-pot synthesis using a single shot addition of 5 mmol of *S*-MBA (carefully added to allow the system to adjust pH) after 180 min was performed and is also shown in Fig. 7. Reasonable agreement was found between the experimental and predicted data for the synthesis with fed-batch addition of MBA shown in Fig. 7. After 2000 min, the consumption rate of MBA by TAm became less than the feed rate of MBA, therefore accumulation of the amino-donor started to occur. No further conversion was obtained after 3200 min; this was probably caused due to enzyme deactivation instead of an equilibrium constraint due to the high equilibrium constant determined for the bioconversion of 843 (Table 2). In the bioconversion with a single shot addition of MBA, as Eq. (2) predicted, the rate of ABT synthesis was initially faster than for the fed-batch bioconversion, resulting in higher ABT yields for the first 1000 min of reaction. Nevertheless, it appears TAm was totally inactivated after 1000 min by the higher concentration of MBA in comparison with the fed-batch bioconversion, and no further production of ABT was measured after that time. The result was a final conversion yield of 62% mol/mol for the bioconversion with fed-batch addition, which was 25% higher than the corresponding yield using the one shot addition of MBA.

3.4.2. *One-pot synthesis of APD with fed-batch addition of IPA*

Although the bioconversions using MBA were determined not to be equilibrium controlled (Table 2), the bioconversions did suffer from toxicity and inhibition problems of the amino-donor. IPA had shown great potential in microscale bioconversions at low substrate concentrations and was therefore selected as a new amino-donor (Rios-Solis et al., 2011). In addition, any excess of IPA added in a fed-batch mode can be easily evaporated due to its high volatility (Smith et al., 2010).

Due to IPA evaporation using the microscale tools, it was not possible to obtain reliable data to determine the kinetic parameters with this substrate, nevertheless because the TAm reaction mechanism is divided into two half reactions, it was assumed that the Michaelis Menten constant of ERY and PKD was still high, and that inhibition and toxicity of the amino donor would still be present. Therefore, a preparative scale, one-pot synthesis of APD was performed with fed-batch addition of IPA. The initial concentration of PA and HPA were 200 mM (20 fold higher than the concentrations used in Fig. 5). The concentration of TK D469E and the CV2025 TAm were 0.75 and 0.14 mg mL^{-1} using a whole cell biocatalyst. Using Eq. (1) and the kinetic parameters from Table 1, it was predicted that the TK reaction would reach completion after 10 h. At that time, a solution of IPA 500 mM was fed continuously at a flow rate of 0.42 mL h^{-1} during 48 h, so that a total amount of 10 mmol of IPA would be added to the vessel equivalent to a normalised concentration of 200 mM in 50 mL. Fig. 8 shows the experimental progress curve for normalised concentrations of HPA, PKD and APD, as well as the predicted data of the TK step (the TAm step was not modelled because the kinetic parameters using IPA were not determined in this work).

Excellent agreement was found between the experimental and predicted TK data using Eq. (1), which validated the TK model for concentrations as high as 200 mM in a preparative scale synthesis. The TAm bioconversion did not seem to be inhibited by any accumulation of IPA during the 3000 min that the amino-donor was fed, suggesting that any excess of IPA evaporated away to below inhibitory levels. A total volume of IPA solution of 20 mL was added to the bioreactor, leading to a final APD yield of 70% mol/mol. This yield was 3.5 fold higher than the yield obtained for similar batch reaction conditions for a single TAm step bioconversion (data not shown). This suggested that fed-batch IPA addition could be overcoming inhibition or toxic effects on TAm activity at high concentrations.

Table 6 shows a summary of the different bioreactor configurations, initial concentrations, amino-donor selection and final yields for the different preparative scale one pot syntheses of APD and ABT. Comparing these results with literature, a previous TK–TAm two step, preparative scale batch synthesis of APD (using 2 bioreactors) had achieved a final product concentration 37.8 mM from a starting TK substrate concentration of 300 mM (12.6% mol/

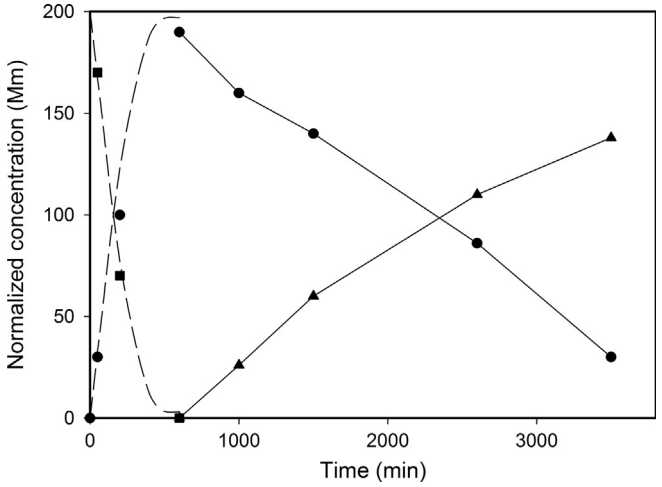

Fig. 8. Typical progress curves for modelling the TK–TAm one-pot synthesis of APD with continuous fed-batch addition of IPA at preparative scale. Concentrations normalised to a reference volume of 50 mL: (■) HPA, (●) PKD and (▲) APD. Initial reaction conditions: 50 mL working volume, 200 mM [HPA] and [PA], 0.2 mM [PLP], 2.4 mM [TPP], 9 mM [Mg^{2+}], 30 °C, pH 7.5, 25 mM HEPES. After 600 min, a solution of 500 mM [IPA] was added with a constant flow rate of 0.42 mL h^{-1}. [TK] and [TAm] were 0.75 and 0.14 mg mL^{-1} respectively in whole cell form. Kinetic profiles (dashed lines) of the TK step were modelled using Eq. (1) with the corresponding kinetic parameters from Table 1.

Table 6
Comparison of the different bioconversion conditions, bioreactor configurations and final yields for the preparative scale one pot syntheses of ABT and APD.

Product synthesis	Reactor configuration	Amino-donor	Initial substrate concentration (mM)	Final yield (% mol/mol)
ABT	Batch	MBA	10	94
APD	Batch	MBA	10	85
ABT	Batch	MBA	100	37
ABT	Fed-batch	MBA	100	62
APD	Batch	IPA	200	19
APD	Fed-batch	IPA	200	70

mol yield) (Smith et al., 2010). In that work 30% of TK intermediate (PKD) was lost due to product isolation, while a lower concentration of TAm substrates had to be used due to inhibition. Those problems were alleviated in this work where no isolation of TK intermediates was needed, and concentrations 1 order of magnitude higher of TAm substrates could be used due to the selected reaction conditions and reactor configuration. This allowed a final product concentration of 140 mM to be attained from initial TK reactant concentrations of 200 mM. This represents a 70% mol/mol conversion and a 6 fold greater yield than in the previous work.

4. Conclusions

The success of synthetic biology relies in great part in the characterisation and integration of the individual synthetic components. For a non-native, multi-enzymatic synthesis, the kinetic modelling of the individual steps is crucial to being able to "mix and match" the best enzymes and determine the best reactor configuration. This needs to be combined with a fine tuning of expression system to achieve the required individual enzyme concentrations. There are practically no studies where those kinetic analyses combined with synthetic biology tools were performed for cascade-type and one-pot catalytic reactions, hence limiting its speed development and application at the industrial scale. The microscale tools used here allowed those tasks to be performed with minimum resources and time, allowing a quantitative prediction of the reaction kinetics and substantial improvements over previously reported yields. Due to the advances in synthetic biology, the development of multi-step, one pot biocatalytic processes will increase and microscale kinetic modelling approaches as shown in this work will be crucial to speed technology translation to industrial scale.

Acknowledgements

The Mexican National Council for Science and Technology (CONACYT), the Mexican Ministry of Public Education (SEP) and the Royal Thai Government are acknowledged for support of Leonardo Rios-Solis and Phattaraporn Morris. The UK Engineering and Physical Sciences Research Council (EPSRC) is thanked for the support of the multidisciplinary Biocatalysis Integrated with Chemistry and Engineering (BiCE) programme (GR/S62505/01) at University College London (London, UK).

References

Bhaskar, G., 2004. A short stereoselective synthesis of (−)-chloramphenicol and (+)-thiamphenicol. Tetrahedron: Asymmetry 15, 1279–1283.
Bulos, B., Handler, P., 1965. Kinetics of beef heart glutamic-alanine transaminase. J. Biol. Chem. 240, 3283.
Cázares, A., Galman, J.L., Crago, L.G., Smith, M.E.B., Strafford, J., Rios-Solis, L., Lye, G.J., Dalby, P.A., Hailes, H.C., 2010. Non-alpha-hydroxylated aldehydes with evolved transketolase enzymes. Org. Biomol. Chem. 6, 1301–1309.
Chen, B.H., Micheletti, M., Baganz, F., Woodley, J., Lye, G.J., 2009. An efficient approach to bioconversion kinetic model generation based on automated microscale experimentation integrated with model driven experimental design. Chem. Eng. Sci. 64, 403–409.
Chen, B.H., Hibbert, E.G., Dalby, P.A., Woodley, J.M., 2008. A new approach to bioconversion reaction kinetic parameter identification. AIChE J. 54, 2155–2163.
Cohen, S.A., Michaud, D.P., 1993. Synthesis of a fluorescent derivatizing reagent, 6-aminoquinolyl-N-hydroxysuccinimidyl carbamate, and its application for the analysis of hydrolysate amino acids via high-performance liquid chromatography. Anal. Biochem. 211, 279–287.
Dalby, P.A., Baganz, F., Lye, G.J., Ward, J.M., 2009. Protein and pathway engineering in biocatalysis. Chim. Oggi 27, 18–21.
Ellis, R.J., Davies, D.D., 1961. Glutamic-oxaloacetic transaminase of cauliflower. 1. Purification and specificity. Biochem. J. 78, 615–623.
Gyamerah, M., Willetts, A.J., 1997. Kinetics of overexpressed transketolase from *Escherichia coli* JM 107/pQR 700. Enzym. Microb. Technol. 20, 127–134.
Halim, M., Rios-Solis, L., Micheletti, M., Ward, J.M., Lye, G.J., 2014. Microscale methods to rapidly evaluate bioprocess options for increasing bioconversion yields: application to the ω-transaminase synthesis of chiral amines. Bioprocess Biosyst. Eng. 37, 931–941.
Hussain, H.A., Ward, J.M., 2003. Enhanced heterologous expression of two *Streptomyces griseolus* cytochrome P450s and *Streptomyces coelicolor* ferredoxin reductase as potentially efficient hydroxylation catalysts. Society 69, 373–382.
Ingram, C.U., Bommer, M., Smith, M.E.B., Dalby, P.A., Ward, J.M., Hailes, H.C., Lye, G.J., 2007. One-pot synthesis of amino-alcohols using a *de-novo* transketolase and β-alanine: pyruvate transaminase pathway in *Escherichia coli*. Biotechnology 96, 559–569.
Kaldor, S.W., Kalish, V.J., Davies, J.F., Shetty, B.V., Fritz, J.E., Appelt, K., Burgess, J.A., et al., 1997. Viracept (nelfinavir Mesylate, AG1343): a potent, orally bioavailable inhibitor of HIV-1 protease. J. Med. Chem. 40, 3979–3985.
Kaulmann, U., Smithies, K., Smith, M.E.B., Hailes, H., Ward, J., 2007. Substrate spectrum of Ω-transaminase from *Chromobacterium violaceum* DSM30191 and its potential for biocatalysis. Enzym. Microb. Technol. 41, 628–637.
Keasling, J.D., 2010. Manufacturing molecules through metabolic engineering. Science 330, 1355–1358.
Kuramitsu, S., Hiromi, K., Hayashi, H., Morino, Y., Kagamiyama, H., 1990. Pre-steady-state kinetics of *Escherichia coli* aspartate aminotransferase catalyzed reactions and thermodynamic aspects of its substrate specificity. Biochemistry 29, 5469–5476.
Kwon, S., Ko, S., 2002. Synthesis of statine employing a general Syn-amino alcohol building block. Tetrahedron Lett. 43, 639–641.
Lye, J.G., Ayazi-Shamlou, J.P., Baganz, F., Dalby, P.A., Woodley, J.M., 2003. Accelerated design of bioconversion processes using automated microscale processing techniques. Trends Biotechnol. 21, 29–37.
McArthur, G.H., Fong, S.S., 2010. Toward engineering synthetic microbial metabolism. J. Biomed. Biotechnol. 2010, 1–10.
Meyer, A., Pellaux, R., Panke, S., 2007. Bioengineering novel in vitro metabolic pathways using synthetic biology. Curr. Opin. Microbiol. 10, 246–253.
Micheletti, M., Lye, G.J., 2006. Microscale bioprocess optimisation. Curr. Opin. Biotechnol. 17, 611–618.
Morris, K.G., Smith, M.E.B., Malcolm, D.T., Turner, J.N., 1996. Transketolase from *Escherichia coli*: a practical procedure for using the biocatalyst for asymmetric carbon–carbon bond synthesis. Tetrahedron: Asymmetry 7, 2185–2188.
Pollard, D.J., Woodley, J.M., 2007. Biocatalysis for pharmaceutical intermediates: the future is now. Trends Biotechnol. 25, 66–73.
Prather, K.L.J., Martin, C.H., 2008. De novo biosynthetic pathways: rational design of microbial chemical factories. Curr. Opin. Biotechnol. 19, 468–474.
Rios-Solis, L., Bayir, N., Halim, M., Du, C., Ward, J.M., Baganz, F., Lye, G.J., 2013. Non-linear kinetic modelling of reversible bioconversions: application to the transaminase catalyzed synthesis of chiral amino-alcohols. Biochem. Eng. J. 73, 38–48.
Rios-Solis, L., Halim, M., Cázares, A., Morris, P., Ward, J.M., Hailes, H.C., Dalby, P.A., Baganz, F., Lye, G.J., 2011. A toolbox approach for the rapid evaluation of multi-step enzymatic syntheses comprising a 'mix and match' *E. coli* expression system with microscale experimentation. Biocatal. Biotransform. 29, 192–203.
Roessner, C.A., Scott, A.I., 1996. Achieving natural product synthesis and diversity via catalytic networking ex vivo. Chem. Biol. 3, 325–330.
Rozwadoska, M.D., 1993. An efficient synthesis of S-(+)-amphetamine. Tetrahedron: Asymmetry 4, 1619–1624.
Sayar, N.A., Chen, B.H., Lye, G.J., Woodley, J.M., 2009a. Modelling and simulation of a transketolase mediated reaction: sensitivity analysis of kinetic parameters. Biochem. Eng. J. 47, 1–9.
Sayar, N.A., Chen, B.H., Lye, G.J., Woodley, J.M., 2009b. Process modelling and simulation of a transketolase mediated reaction: analysis of alternative modes of operation. Biochem. Eng. J. 47, 10–18.
Shin, J.S., Kim, B.G., 1998. Kinetic modeling of ω-transamination for enzymatic kinetic resolution of α-methylbenzylamine. Biotechnol. Bioeng. 60, 534–540.
Shin, J.S., Kim, B.G., 2002. Exploring the active site of amine:pyruvate aminotransferase on the basis of the substrate structure–reactivity relationship: how the enzyme controls substrate specificity and stereoselectivity. J. Org. Chem. 67, 2848–2853.
Sin, G., Woodley, J.M., Gernaey, K.V., 2009. Application of modeling and simulation tools for the evaluation of biocatalytic processes: a future perspective. Biotechnol. Prog. *25*, 1529–1538.
Smith, M.E.B., Chen, Bing H., Hibbert, E.G., Kaulmann, U., Smithies, K., Galman, J.L., Baganz, F., et al., 2010. A multidisciplinary approach toward the rapid and

preparative-scale biocatalytic synthesis of chiral amino alcohols: a concise transketolase-/ω-transaminase-mediated synthesis of (2*S*,3*S*)-2-aminopentane-1,3-diol. Org. Process Res. Dev. 14, 99–107.

Sprenger, G.A., Schörken, U., Sprenger, G., Sahm, H., 1995. Transketolase A of *Escherichia coli* K12. Purification and properties of the enzyme from recombinant strains. Eur. J. Biochem./FEBS 230, 525–532.

Truppo, M.D., Rozzell, J.D., Moore, J.C., Turner, N.J., 2009. Rapid screening and scale-up of transaminase catalysed reactions. Org. Biomol. Chem. 7, 395–398.

Van Ophem, P.W., Erickson, S.D., Martinez del Pozo, A., Haller, I., Chait, B.T., Yoshimura, T., Soda, K., Ringe, D., Petsko, G., Manning, J.M., 1998. Substrate inhibition of D-amino acid transaminase and protection by salts and by reduced nicotinamide adenine dinucleotide: isolation and initial characterisation of a pyridoxo intermediate related to inactivation. Biochemistry 37, 2879–2888.

Watson, J.D., 1972. Molecular Biology of the Gene, second ed. Saunders, Philadelphia, PA.

Woodley, J.M., 2006. Choice of biocatalyst form for scalable processes. Biochem. Soc. Trans. 34, 301–303.

Xue, R., Woodley, J.M., 2012. Process technology for multi-enzymatic reaction systems. Bioresour. Technol. *115*, 183–195.

Yun, H., Cho, B.K., Kim, B.G., 2004. Kinetic resolution of (R,S)-sec-butylamine using omega-transaminase from *Vibrio fluvialis* JS17 under reduced pressure. Biotechnol. Bioeng. 87, 772–778.